COMPUTER SIMULATION AND COMPARISON OF PROTON AND CARBON ION TREATMENT OF TUMOR CELLS USING PARTICLE AND HEAVY ION TRANSPORT CODE SYSTEM

A Thesis

by

KEEL BRANDON CURTIS

Submitted to the Office of Graduate Studies of
Texas A&M University
in partial fulfillment of the requirements for the degree of

MASTER OF SCIENCE

December 2010

Major Subject: Health Physics

COMPUTER SIMULATION AND COMPARISON OF PROTON AND CARBON ION TREATMENT OF TUMOR CELLS USING PARTICLE AND HEAVY ION TRANSPORT CODE SYSTEM

A Thesis

by

KEEL BRANDON CURTIS

Submitted to the Office of Graduate Studies of
Texas A&M University
in partial fulfillment of the requirements for the degree of

MASTER OF SCIENCE

Approved by:

Chair of Committee,	Stephen Guetersloh
Committee Members,	Leslie A. Braby
	John Ford
	Benjamin Young
Head of Department,	Raymond J. Juzaitis

December 2010

Major Subject: Health Physics

ABSTRACT

Computer Simulation and Comparison of Proton and Carbon Ion Treatment of Tumor Cells Using Particle and Heavy Ion Transport Code System. (December 2010)

Keel Brandon Curtis, B.S., Texas A&M University

Chair of Advisory Committee: Dr. Stephen Guetersloh

Charged particle beams are an increasingly common method of cancer treatment. Because of their Bragg peak dose distribution, protons are an effective way to deliver a dose to the tumor, while minimizing the dose to surrounding tissue. Charged particles with greater mass and higher charge than protons have an even sharper Bragg peak and a higher Relative Biological Effectiveness (RBE), allowing a greater dose to be delivered to the tumor and sparing healthy tissue. Since carbon ions are being implemented for treatment in Europe and Japan, this study will focus on carbon as the heavier ion of choice. Comparisons are drawn between moderated and unmoderated protons and carbon ions, all of which have a penetration depth of 10 cm in tissue. Scattering off the beam line, dose delivered in front of and behind the tumor, and overall dose mapping are examined, along with fragmentation of the carbon ions.

It was found that fragmentation of the carbon ion beam introduced serious problems in terms of controlling the dose distribution. The dose to areas behind the tumor was significantly higher for carbon ions versus proton beams. For both protons and carbon ions, the use of a moderator increased the scattering off of the beam line, and slightly increased the dose behind the tumor. For carbon ions, the use of a moderator increased the degree of fragmentation throughout the beam path.

TABLE OF CONTENTS

LIST OF FIGURES

LIST OF TABLES

1. INTRODUCTION

Radiation is one of the major forms of treatment for tumors available today. Radiation is used in curing 23% of all cancers, either alone or in combination with chemotherapy or surgery (IAEA/ICRU 2008). The oldest type of radiation therapy is simple irradiation of a tumor with x-rays, first used more than 100 years ago (Early and Landa 1995). By passing x-radiation through the tumor, doctors hope to deposit enough energy within to kill cells, halting or reversing the tumor's growth. The deposition of energy by radiation is called a dose, and is typically given in Gray (Gy); 1 Gy is 1 joule per kilogram. However, two notable properties of x-rays are their tendency to scatter, and their exponential attenuation. Because they are effectively weightless, x-ray photons can scatter at large angles from the beam easily. This can lead to dose being delivered far away from the target. X-rays attenuate exponentially because their interactions with target atoms are random. The interaction rate is tied to the number of photons present. As they travel through a material, photons interact and lose energy, and are eventually absorbed. Thus, the number of photons, as well as the dose they deliver, decreases exponentially with depth. Both of these characteristics lead to dose and damage within healthy tissue, which limits the maximum dose that can be safely delivered to a tumor. The more dose that can be delivered to a tumor, the greater the likelihood of controlling the tumor, stopping its growth or even shrinking it. Any treatment that can deliver a greater portion of dose to the tumor instead of healthy tissue is desirable.

In 1946 Robert Wilson proposed using protons for tumor treatment. (Schulz-Ertner and Tsujii 2007) Unlike uncharged photons, positively charged protons primarily slow down through many Coulomb interactions with the positive nuclei and negative electrons comprising a target material. (Attix 2004) Each interaction transfers a small amount of energy from the incident particle to the medium through which it is

---

This thesis follows the style of Health Physics.

travelling. This is known as a "soft" collision. Occasionally, the incident particle will come closer to a particular atom and interact with an orbiting electron, a "hard" collision, transferring enough energy to eject the electron from its shell as a delta ray. These delta rays are low energy, and appear as short-ranged spurs from the main particle track. Together, these two types of interaction sum to give the total stopping power, the differential energy lost per unit distance travelled through a material. Stopping power is closely related to Linear Energy Transfer (LET), the amount of energy transferred to the medium being traversed per unit length. Stopping power is given by eqn (1):

$$\left[{}^{dE}/_{\rho dx}\right]_{total} = \left[{}^{dE}/_{\rho dx}\right]_{hard} + \left[{}^{dE}/_{\rho dx}\right]_{soft} \tag{1}$$

As shown above, stopping power is often given as Mass Stopping Power, ${}^{dE}/_{\rho dx}$, in an effort to normalize materials of different densities, effectively setting them to the same mass. By inserting approximations for the hard and soft terms, and combining constants, such as electron radius, mass, the speed of light, and others, we can reach a form of eqn (1) more useful for computation, as presented in eqn (2):

$$\left[{}^{dE}/_{\rho dx}\right]_{total} = 0.3071\frac{Zz^2}{A\beta^2}\left[13.8373 + \ln\left(\frac{\beta^2}{1-\beta^2}\right) - \beta^2 - \ln I\right] \tag{2}$$

where

Z=atomic number of the target material
z=atomic number of the particle
A=atomic mass of the target material
β=velocity of the particle as a fraction of the speed of light
I=mean excitation potential of the medium, in eV.

The atomic composition of the material is important in this equation. The *Z/A* factor for the target material is directly proportional to the number of electrons per

unit mass. Mass stopping power increases with more electrons per unit mass. Z/A is unity for hydrogen, and is less than 0.5 for other elements, decreasing slowly as Z increases. The mean excitation potential is a mean value of all the ionization and excitation potentials of a particular atom or compound. It is given in electron volts (eV), the amount of energy gained by an electron as it crosses a 1 volt potential. The conversion factor for is 1 eV = 1.602×10^{-19} J; units of keV (1,000 eV) and MeV (1,000,000 eV) are also commonly used. The factor -ln I also decreases mass stopping power slowly with increasing Z. Because the materials in this experiment are unchanging, these factors will remain constant.

The projectile particle's charge and velocity are also factors. Velocity is given as the fraction of the speed of light that the particle is traveling, $\beta = v/c$. Thus, β is unitless. As β is in the denominator, stopping power decreases with increasing β, so higher velocity particles have lower stopping power. Stopping power increases with the square of charge or atomic number (z). For example, an alpha particle, z=2, has a stopping power 4 times greater than a single proton, z=1, at the same velocity. Stopping power does not depend directly on the particle's mass. However, given equal total energies, a heavier particle has a lower velocity than a lighter particle. Discussing particle energies on a per-nucleon basis equates energy to equal velocities and we can more easily compare them.

Because of these differences in the way they lose energy, protons and heavier ions behave very differently from photons as they travel through materials. At the end of their tracks, the stopping power of protons increases dramatically. This leads to a phenomenon known as the Bragg peak. When dealing with particles more massive and highly charged than protons, such as helium nuclei or carbon nuclei, the increase in LET at the end of the track is even more pronounced. The differing energy loss profiles of photons, protons, and carbon ions are shown in Fig. 1.

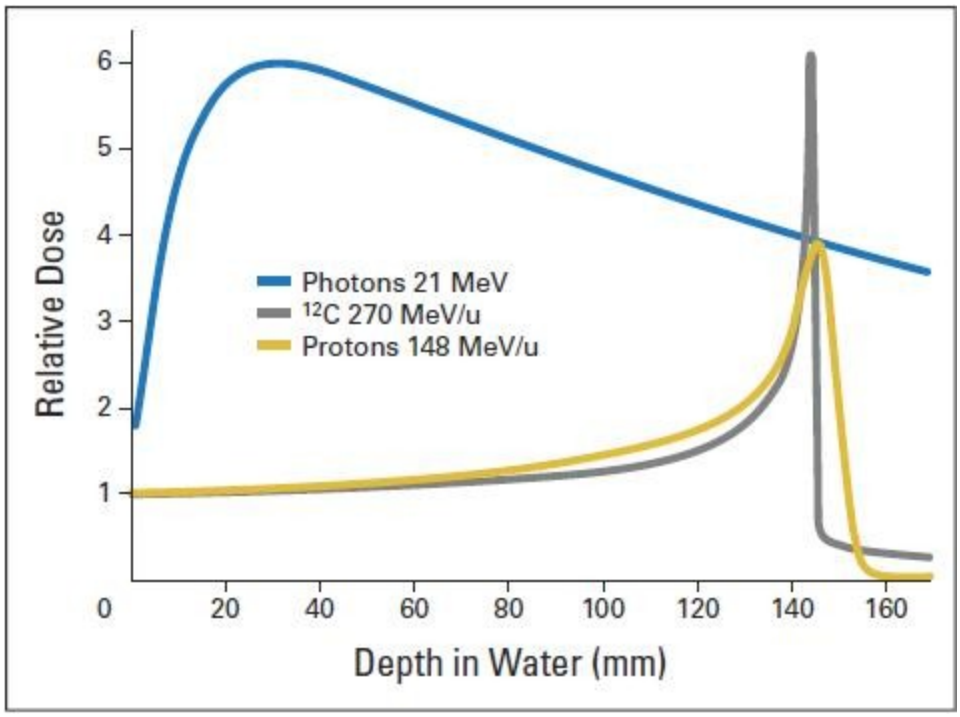

Fig. 1. A Typical Bragg Peak for Protons and Carbon. The proton and photon curves are normalized to show the same dose at 145 mm. The carbon ion curve is normalized to give the same entrance dose as protons. Photons deliver more dose to areas in front of the target than the target itself. Carbon ions can deliver 50% more dose at the target than protons with an equal entrance dose. (Schulz-Ertner and Tsujii 2007)[1]

As shown in Fig. 1, photons have a high entrance dose, peaking at 2-3 cm depth. The dose falls off exponentially afterwards, reaching about 60% of the maximum at the target depth. The maximum usable dose of radiation for cancer treatment is limited by the dose to healthy tissue. One way to control dose to healthy tissue is to use multiple x-ray beams from different angles, also known as ports. The x-ray beams are aimed so that the tumor is the target for each one, but each beam travels through different sections of healthy tissue. For example, instead of using a single beam, two beam ports

[1] Reprinted with permission. © 2008 American Society of Clinical Oncology. All rights reserved.

each delivering half of the dose would be used. The dose to the tumor remains the same; the dose to healthy tissue is reduced by half.

Fig. 1 also shows the dose distributions for charged particles, in this case protons and ^{12}C ions. At the end of their range both exhibit the steep increase in energy deposition known as a Bragg peak. For equal doses at 140 mm depth, protons give a much lower entrance dose than photons. Using carbon ions with the same entrance dose as protons, the dose at 140 mm is increased by 50% and the peak is narrower. Fig. 1 also shows that the charged particle dose deposition drops off very quickly as the ion stops completely after the peak, unlike a photon beam that continues to travel and deliver dose through the medium.

Though they show favorable dose deposition profiles, heavy ions such as carbon can also fragment, which is not possible for either photons or protons. Fragmentation is the breakup of the initial particle breaks into smaller particles. Carbon, with a *Z* of 6, could fragment into two particles with *Z*=2 (helium) and *Z*=4 (beryllium), for example. This presents complications for ion use in therapy. If the ions did not fragment, their energy deposition would drop sharply to zero at the end of their range much like protons, as shown in Fig. 1. However, lower-*Z* secondary fragments have longer ranges than the primary particles for a given velocity. These fragments are then able to deliver dose beyond the tumor. The straggling effect of fragmentation increases with increasing *Z*. (Schardt et al. 1996)

In addition to fragments, charged particles, (including protons) create delta rays. As they travel, charged particles transfer energy to atoms of the target material. Much of this energy is transferred to electrons. Electrons that receive enough energy can leave their parent atom as a delta ray. The more energy imparted to a delta ray, the longer its range. Therefore carbon, at the same energy per nucleon as a proton, has the potential to produce many more delta rays carrying energy away from the intended path. Delta rays can also create photons in their own interactions with the target material. These photons also carry energy away from the charged particle track.

1.1 Radiation Biology

When energy is transferred to living cells, harmful effects may occur. The most harmful effect, to healthy tissue and tumors, is damage to DNA (Hall and Giaccia 2006). All cells have repair mechanisms to detect and fix damage done by radiation and other insults. (Hall and Giaccia 2006) However if these mechanisms make errors, or are overwhelmed by severe and widespread damage, the changes in DNA can be permanent. These mutations can impair the cell's ability to grow and reproduce, or even kill it outright. Unrepaired DNA can also be passed on to daughter cells, creating a new generation of mutant cells. All of these effects are undesirable in healthy tissue, but are the key to shrinking and killing tumors.

Compared to protons, heavy ions (Z>2) have an increased relative biological effectiveness (RBE) when causing changes in cells (IAEA/ICRU 2008). RBE is a comparison of two different types of radiation, typically high and low LET. To measure RBE, two types of radiation are used to achieve the same endpoint, 50% cell death for example, with x-ray or gamma exposures being the reference radiation. This will occur at a different dose for each type. Then the low-LET dose is divided by the high-LET dose, and this gives a ratio. This ratio is the RBE of the high-LET radiation compared to the low-LET. In this report, the RBE endpoint is tumor cell inactivation, unless otherwise mentioned.

Dose multiplied by quality factor is effective dose. Quality factor is closely related to and often drawn from RBE. This allows easier comparison of different doses that should have similar biological effects. The unit for effective dose is the Sievert (Sv) which is equal to 1 Gy at a quality factor of 1.

Effective cancer control requires that radiation does enough damage to DNA to cause the cancer cell to die or stop reproducing. Because DNA is comprised of two strands, it can be damaged by either single or double strand breaks (SSB, DSB respectively), among other types of damage. A DSB is a complete cut across a segment of DNA, and is harder for a cell to repair than other types of damage. Photons cause

damage in a very spread out pattern. High-LET radiation is more likely to cause complex damage because of nuclear interactions and the dense delta ray cloud surrounding the track. (Durante and Cucinotta 2008) Complex damage is when multiple DSBs, SSBs or other damage occur in a small section of DNA. Complex damage is extremely hard to repair properly.

Cancer cells often have poorly-functioning repair mechanisms compared to healthy cells. (Rusin et al. 2009) This leads to a program of dose fractionation. Instead of one large dose, a cancer patient is given smaller daily doses over the course of a few weeks. Cancer cells often have a poor system to halt cell growth and division compared to healthy cells. Fractionation allows healthy cells to halt cell growth and repair, while cancer cells are more likely to try and grow with damaged DNA. These cells are more likely to experience cell death or an inability to continue growth and division. (Pawlik and Keyomarsi 2004)

1.2 Carbon Ions

As shown in Fig. 1 the Bragg peak for carbon ions is even sharper and narrower than that of protons. In addition, carbon ions have a higher RBE at the end of their tracks. While protons have an RBE of about 1.1, values for carbon go as high as 4. (Schulz-Ertner and Tsujii 2007) Additionally, being a much more massive nucleus, carbon scatters much less. Many researchers have taken these as reasons to believe that heavy ions are even more precise and effective than protons for beam therapy. While higher-*Z* particles offer even higher LET values at the end of their tracks, they also suffer from a greater degree of fragmentation, increasing the relative dose beyond the Bragg peak. Also, at higher LET values, the RBE begins to decrease, as overkill effects come into play. Overkill is when the radiation is so damaging that it has a 100% kill rate for cells it enters. Further increasing the energy deposition does not do any more damage and the excess energy is 'wasted'. Thus, carbon and oxygen beams have been focused on as possible therapy beams though debate continues as to whether the

benefits of heavier nuclei outweigh the problems that fragmentation poses. (Schardt et al. 1996)

Furthermore, the cost of accelerators to produce heavy ions is higher than the cost of a proton accelerator. Because of the very narrow Bragg peak, imaging and delivery systems also need to be more precise for heavy ion treatment. Thus, the overall cost is significantly higher; this has limited their use in research studies and patient treatment. However, some heavy ion trials in Germany and Japan have been conducted using carbon. The results have been promising, with a high degree of local control, and minimal side effects. (Shulz-Ertner 2003, Imai et al. 2004) The expected cost for a typical proton therapy center was about $125 million in 2009. (Huff 2007) The expected cost for a carbon therapy center is between $200 and $300 million in 2009, though this may be reduced greatly for subsequent centers. (Zamosky 2009, Yamada 2007) As of March 2009, only 5342 patients worldwide have been treated with carbon therapy, compared to over 60,000 with protons. There are only 3 facilities, 2 in Japan, 1 in Germany, that currently offer carbon ion treatments, while 26 facilities, including some in the U.S., offer treatment with protons. Carbon ions need more biological studies, clinical trials and availability if their usefulness and cost-effectiveness are to be proven.

1.3 Simulation

In order to investigate the behavior of both protons and carbon ions the program Particle and Heavy-Ion Transport code System (PHITS) was used. PHITS was developed in collaboration by the Research Organization for Information Science and Technology (RIST), Tohoku University, and Japan Atomic Energy Institute. (Niita 2006)

The code takes the incident particle's energy, direction, and type, and uses known probabilities to simulate its interaction with matter. PHITS is similar in design to MCNP (Monte Carlo N-Particle code), a program that focuses primarily on neutral particles such as photons and neutrons, but PHITS simulates charged particle

interactions such as energy deposition, fragmentation, and ionization and excitation of target atoms. To run PHITS, an input file is created with several sections. The PHITS program parses this input file, runs the simulation within, and creates several output files based on what is called for in the input file.

The first section of the input file contains global variables. This section contains references to data libraries to be used and defines the number of particles to be 'run'. PHITS creates particles one at a time, simulating interactions based on the probability of those interactions occurring given the particle's energy and other factors. It follows the primary particle and the secondary particles created by the primary, until the particles fall below their energy cutoff value. These cutoff values are also defined in the first section of the input file. By increasing the number of particles and decreasing the cutoff values, so they are followed farther, the user can increase the precision of the PHITS output data. However, this also increases the computing time required. It is necessary to strike a balance between accurate data and reasonable computing time.

The next section is a beam definition. Here the type of particle and energy are defined. The shape and size of the beam are also set, as well as its direction. The following two sections are surfaces and cells. Surfaces are simple geometric shapes, such as planes, cylinders, and spheres. These surfaces are combined to create cells. Cells must be completely closed, and are given a material definition. The user can create spheres of water, cylinders of air, rectangular boxes of soft tissue, or more complex creations.

The last sections are called tallies. These extract data from the simulation that is being run and create output files. Tallies can tell how many particles entered a certain cell, how much energy they deposited, and more. Correctly using tallies is crucial to getting useful data out of PHITS.

2. EXPERIMENTAL SETUP

In order to test the effectiveness of carbon ions for treatment, they were compared to proton beams with the same range in tissue. The simulation environment is a simple tissue-equivalent plastic cylinder, 10cm in radius. Tissue equivalence means that radiation entering the material is expected to interact and slow down in a very similar fashion to radiation entering human soft tissue. The atomic composition of the tissue substitute used is given in Table 1.

Table 1. Atomic Composition of A-150 Plastic. (Smathers et al. 1977)

Element	**Abundance**
Carbon	76.8%
Hydrogen	10.2%
Oxygen	5.9%
Nitrogen	3.6%
Calcium	1.8%
Fluorine	1.7%

At the center of the tissue cylinder is a 1 cm cube, representing the tumor target. A sequential series of small boxes, composed of the same plastic, extends beyond the tumor cell. These are used in a tally to score dose to regions behind the tumor. A similar line of boxes extends perpendicular to the beam line. These are also used for dose deposition radially from the tumor. The setup is shown in Fig. 2.

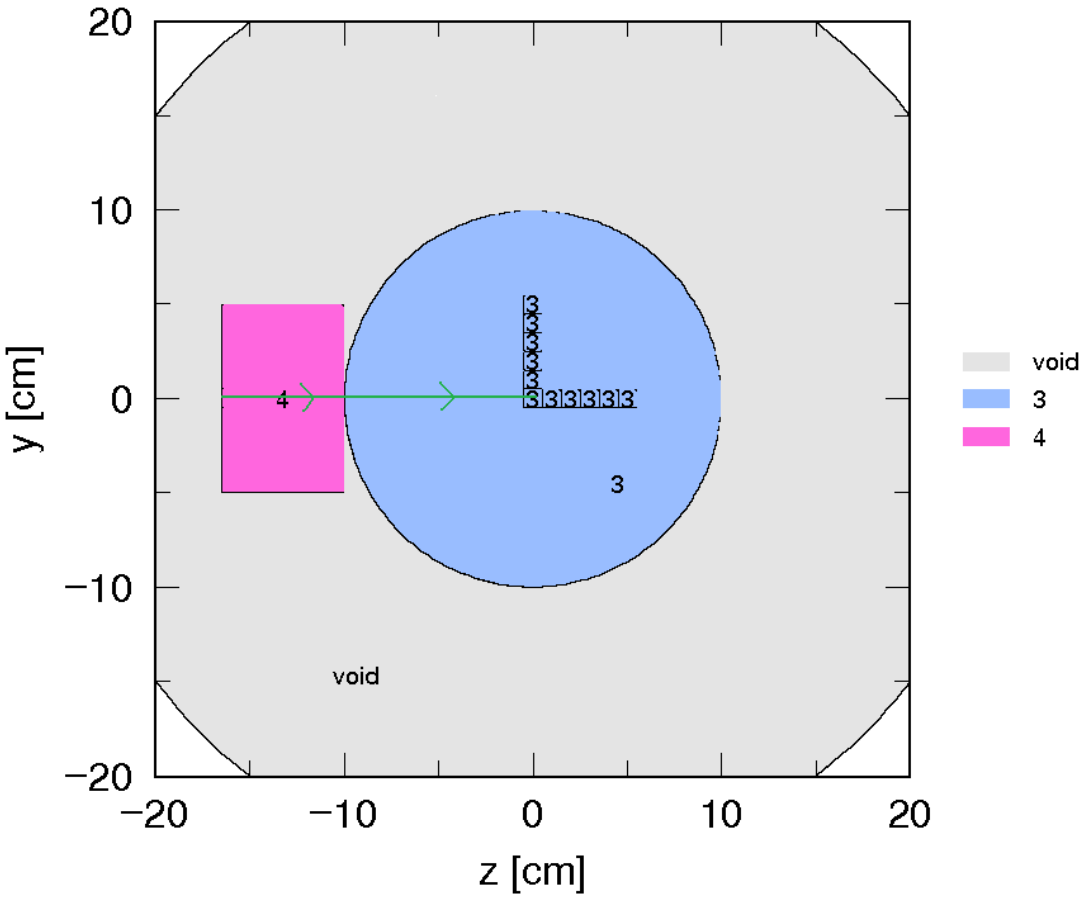

Fig. 2. Experimental Setup. The blue circle is the A-150 plastic cylinder. The pink rectangle shows the polyethylene moderator used in some of the simulations. The green line represents the beam. The L shape of boxes is a series of small cells for the purpose of taking tallies along the beam line behind and perpendicular to the beam line.

Many ion treatment protocols provide ions of the desired energy and range by passing a high-energy ion beam through a moderator before it hits the tissue. By choosing the proper thickness, the reduced-energy ions leaving the moderator then have the proper range to reach the target area. A more advanced technique is to use the accelerator to vary the initial energy of the beam, releasing it when it has reached the desired energy. These two techniques are represented by simulations run with and without a moderator. The moderated simulations used a 6.5 cm block of polyethylene

(CH_2) between the beam and the tissue. The beams being compared are given in Table 2.

Table 2. Beam Types and Initial Energies.

Particle Type and Energy	Moderator Presence
Carbon 290 MeV/u	Moderated
Carbon 219 MeV/u	Unmoderated
Proton 155 MeV	Moderated
Proton 117 MeV	Unmoderated

A total of 4 different beams were run, 2 different particle types, and a moderated and unmoderated run for each particle type. A moderated 290 MeV/u carbon ion beam is typical for use in therapy. After the energy is degraded with a 6.5 cm moderator, it has a range of 10 cm in tissue. The other beams are given initial energies such that their range will also be 10 cm in tissue. The unmoderated beams represent the case of using the accelerator itself to select for the correct energy, and therefore range. They have a lower initial energy but do not pass through a moderator, giving them the same range as the moderated beams. In all cases the beam was a 0.1cm radius pencil beam, starting 7 cm away from the surface of the tissue cylinder. The diameter of the beam was kept small even for the case of the moderated treatments, which are usually the size of the tumor to be treated, so an assessment of lateral divergence could be compared. To reduce statistical uncertainty while preserving a reasonable run time, the number of particles simulated was 400,000. The runtime for each simulation was around 16 hours, with cutoff energies of 0.1 keV for most particles.

3. RESULTS

For each experimental setup, a 2d color plot of energy deposition within the tissue cylinder was created using a 2-dimensional output that maps magnitude to a color scale. Because this material has unit density (1 gm/cm^3) this means energy deposition is directly proportional to dose per particle. If a standard number of particles were picked, multiplying the energy deposition per particle by the number of particles would give a dose map. Figs. 3-6 are essentially blown-up images of the blue circle in Fig. 2.

In Fig. 3, the carbon beam stops at (0,0), but the orange shadow shows fragments continuing to travel through the tissue. The beam is thicker than the unmoderated carbon beam, shown in Fig. 4, but narrow compared to the proton beams, shown in Figs. 5-6. Compared to the other beams, moderated carbon also has the highest overall dose to the entire area.

By eliminating the moderator, the dose away from the beam line is noticeably decreased in Fig. 4. Individual tracks can even be seen near the front of the tissue cylinder. The dose is similar along the line of the treatment beam, but drops off rapidly with distance radially away from the line. The red line showing the highest dose deposition due to carbon ions or fragments, instead of delta rays, is narrower than the moderated beam. The dose behind the tumor is also slightly decreased, but still significant.

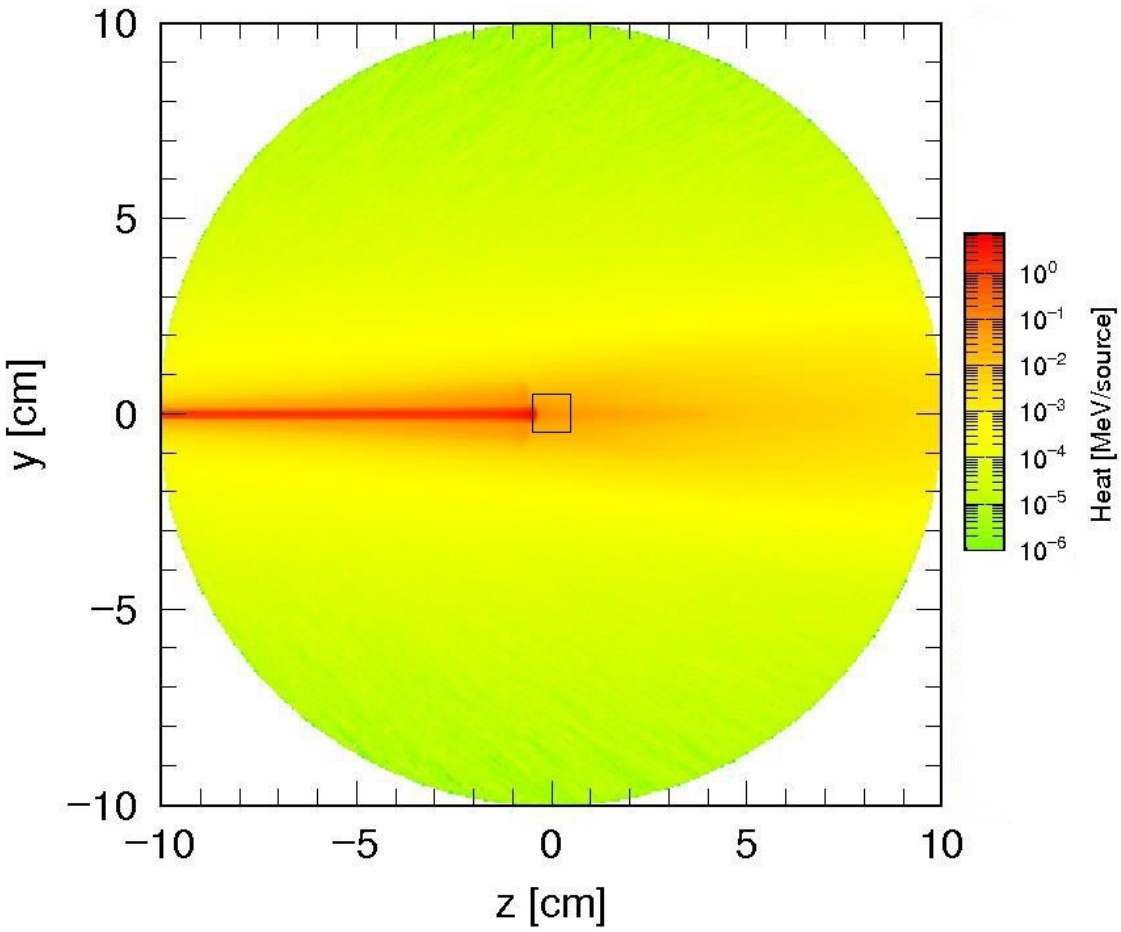

Fig. 3. Moderated Carbon 2d Dose Plot. The tumor target is located in the center of this plot, at (0,0). Energy deposition is in a logarithmic color scale. The beam path is visible as a red line on the left half of the figure. The experimental tumor volume is the small box in the center. Heat is a PHITS term for energy deposited in a region per source particle emitted. Because the target material is unit density, in Figs. 3-6, heat is directly proportional to dose.

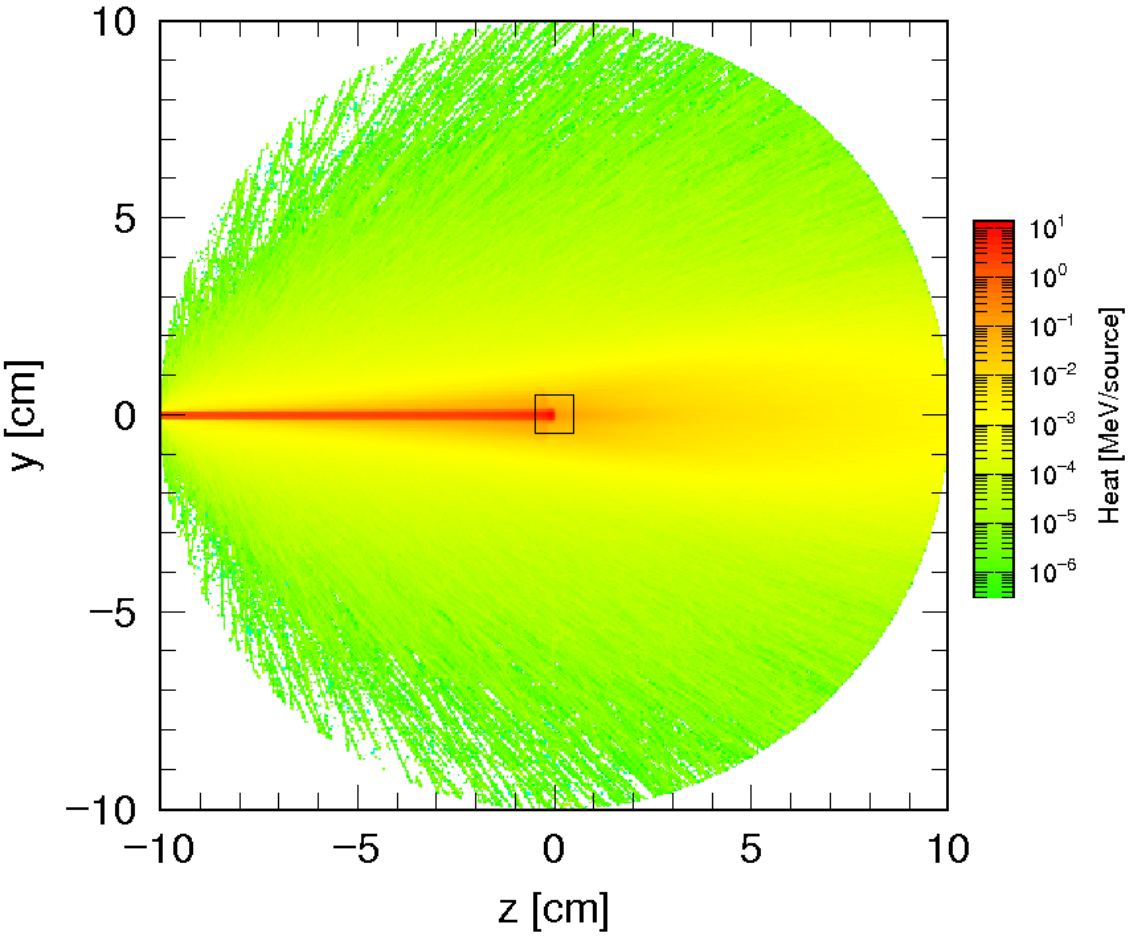

Fig. 4. Unmoderated Carbon 2d Dose Plot. This carbon beam does not pass through a moderator so it does not begin slowing down and scattering until it enters the tissue cylinder.

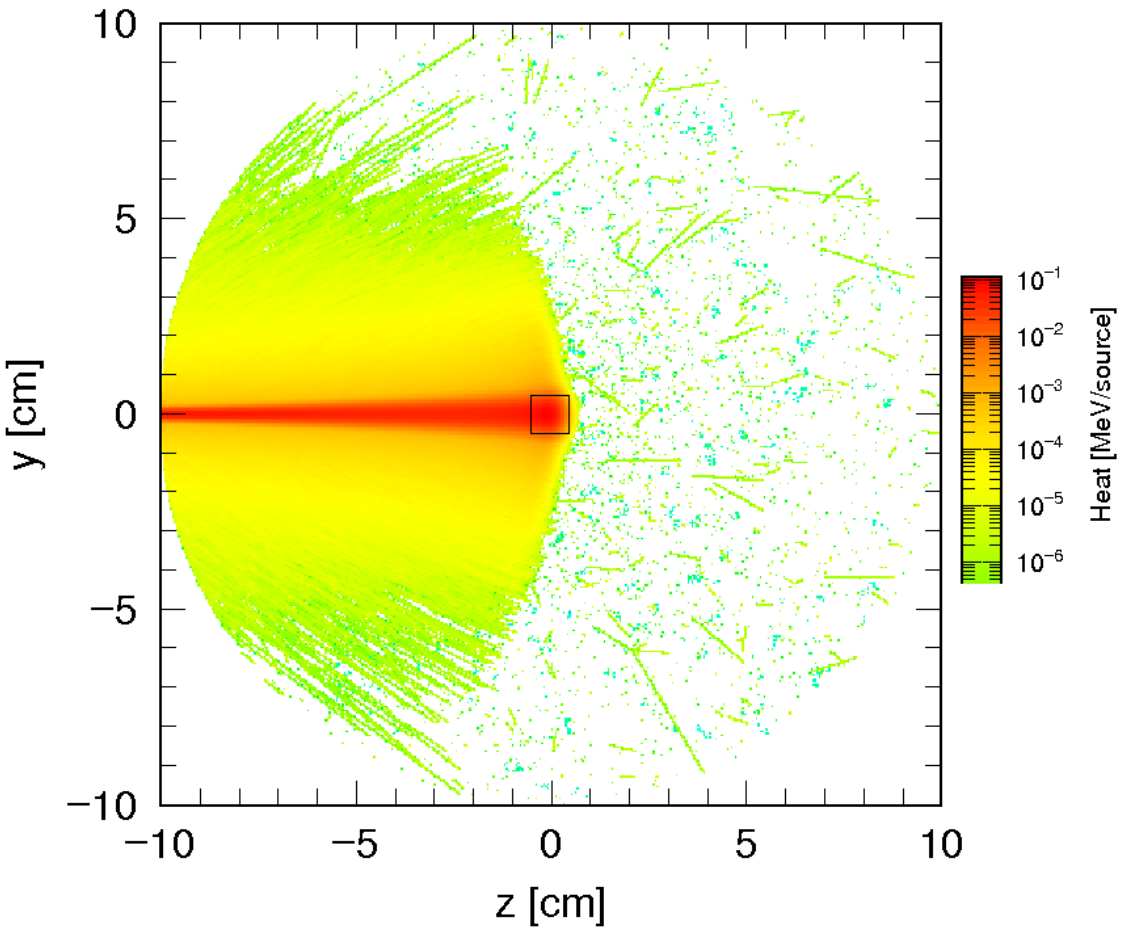

Fig. 5. Moderated Proton 2d Dose Plot. This proton beam is passed through a 6.5 cm moderator before entering the tissue cylinder. Because protons cannot fragment, the energy deposition behind the tumor is practically zero.

Only the sporadic tracks of delta particles and photons are visible past the tumor. However, the dose to areas in front of the tumor is greater than in Figs. 3 and 4. The red area of greatest dose is much thicker for proton therapy, especially at the end near the tumor. The orange area of next highest dose around the beam line is also thicker. Scattering has increased the dose to all areas in a wide path in front of the tumor.

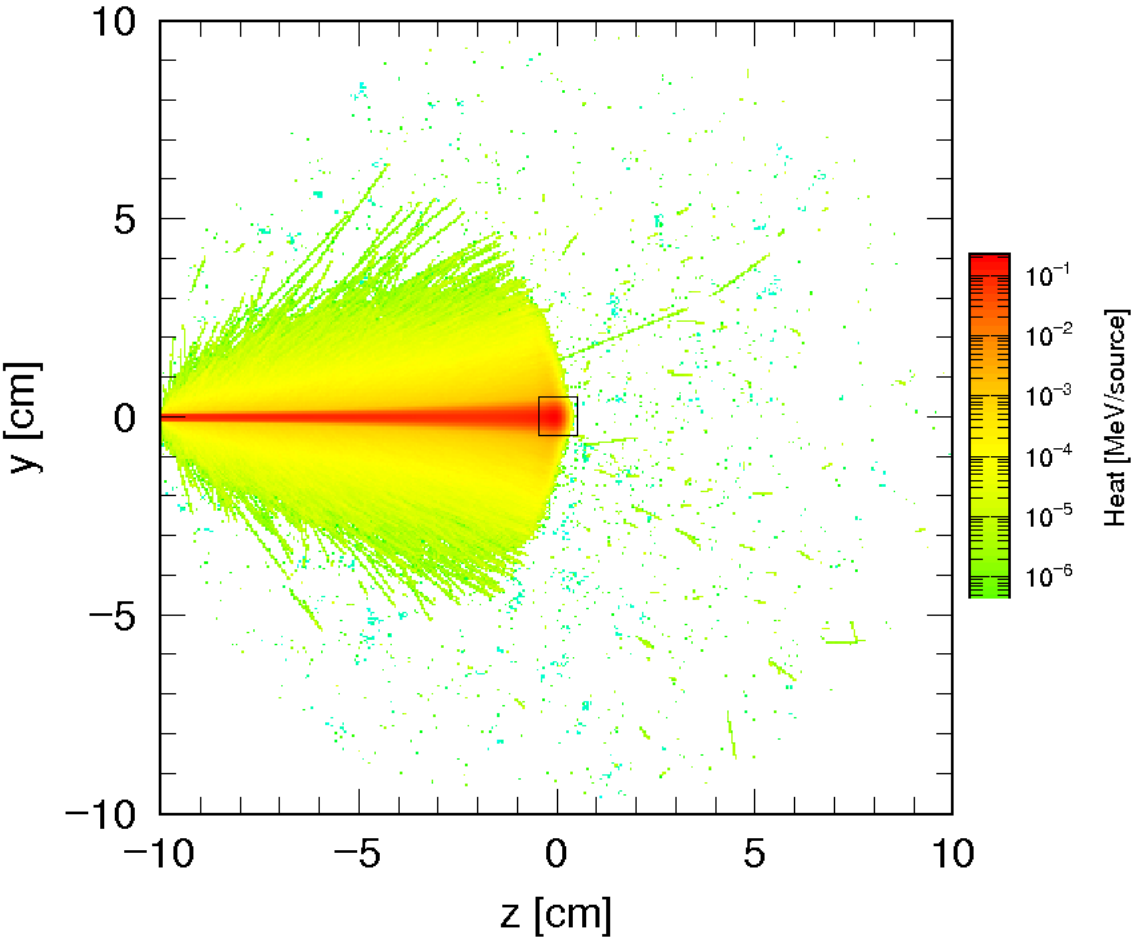

Fig. 6. Unmoderated Proton 2d Dose Plot. This proton beam does not pass through a moderator. Scattering is greatly reduced as a result.

When the moderator is eliminated, the dose conforms more tightly to the beam path. The beam line is thinner, as is the orange area around it. Overall the red line of the beam is comparable to the moderated carbon beam shown in Fig. 3. Scattering far off the beam line is decreased greatly. Again the dose is almost zero past the target, showing only delta particles and photons.

Another set of tallies was used to compare doses in the sequential 1cm^3 cubes behind the tumor target. This shows how the dose falls off beyond the range of the primary particles. The PHITS tallies give results in MeV/source particle. This means that for every particle created, that much energy was deposited in the region of interest. Dose is energy per unit mass and since the mass of the region is known, finding the energy needed to achieve a certain dose is simple:

$$Dose = \frac{energy}{particle} \times numberof\ particles \div mass \qquad (3)$$

By setting the desired dose to the tumor region to 5 Gy, the number of source particles needed for that dose can be calculated using eqn (3). 5 Gy was chosen as a median dose, many studies showed both lower and higher doses delivered to tumors. (Souhami et al. 1991, Krishnanan et al. 2005) This same number of particles was then used for the regions behind the tumor, showing the dose delivered behind the tumor for a 5 Gy dose directly to the tumor. This allowed easier comparisons between proton and carbon ion beams, since carbon beams deposit more energy per particle. The initial runs with 400,000 particles were scaled up to correct for the proper fluence to deliver a 5 Gy dose. The number of particles required to give a dose of 5 Gy to the tumor for each case are given in Table 3.

Table 3. Number of Particles Required to Reach a 5 Gy Tumor Dose.

Trial	Number of Particles
Carbon with Moderator	1.01×10^9
Carbon without Moderator	2.51×10^8
Proton with Moderator	5.19×10^9
Proton without Moderator	4.46×10^9

Fig. 7 shows the results of multiplying the dose/particle number by the number of particles needed for 5 Gy.

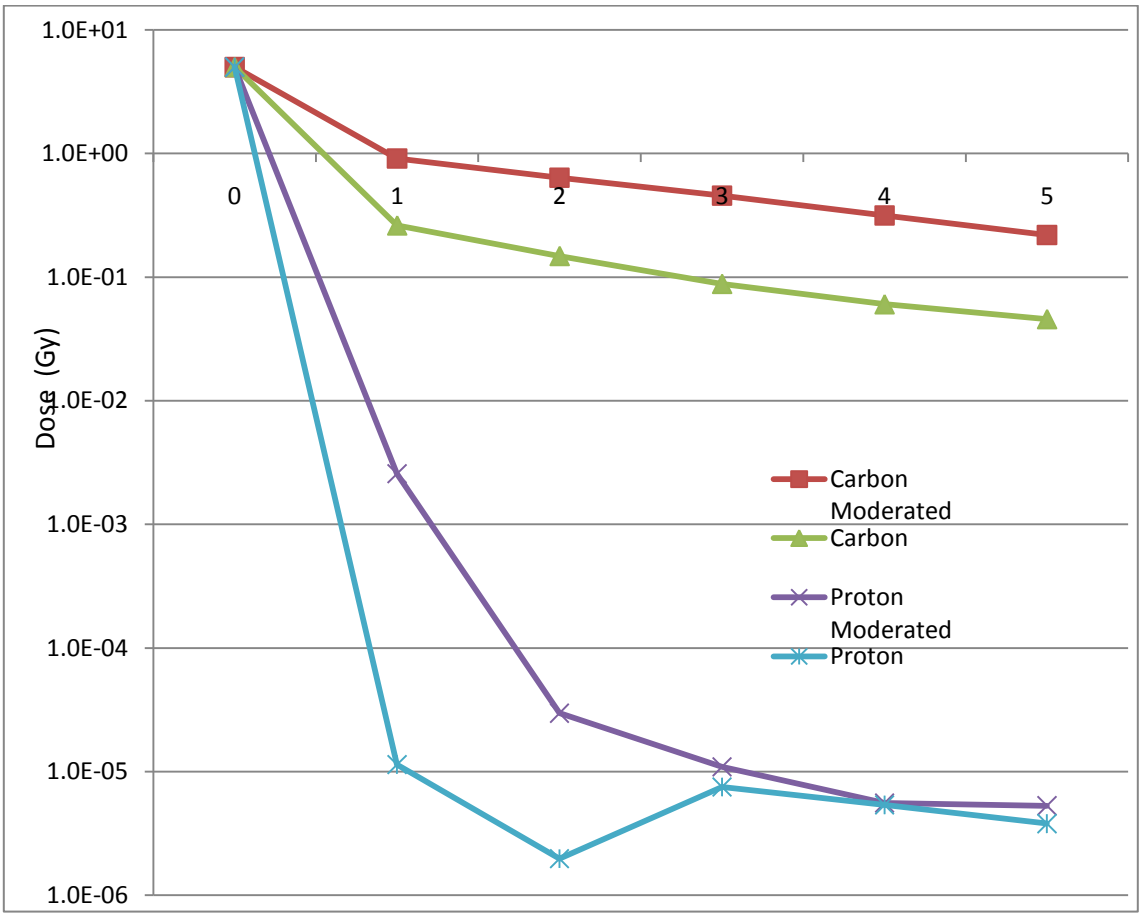

Fig. 7. Dose Delivered Behind the Tumor. 0 is the tumor volume, while 1-5 are cells 1-5cm behind the tumor along the beam line.

The dose from both proton beams drop very quickly behind the tumor. After 1 cm, the dose is decreased by 5 orders of magnitude from the tumor. The only dose at that point is due to delta rays and photons created near the end of the protons' tracks. The carbon ion drops are not nearly as a steep. At 3 cm behind the tumor, the moderated carbon dose is still 0.457 Gy. The unmoderated dose at 3 cm is 0.08 Gy.

The same analysis was done for regions beside the tumor, perpendicular to the beam line. Dose was normalized to 5 Gy, and regions from 1-5 cm away from the tumor were scored. The results are in Fig. 8.

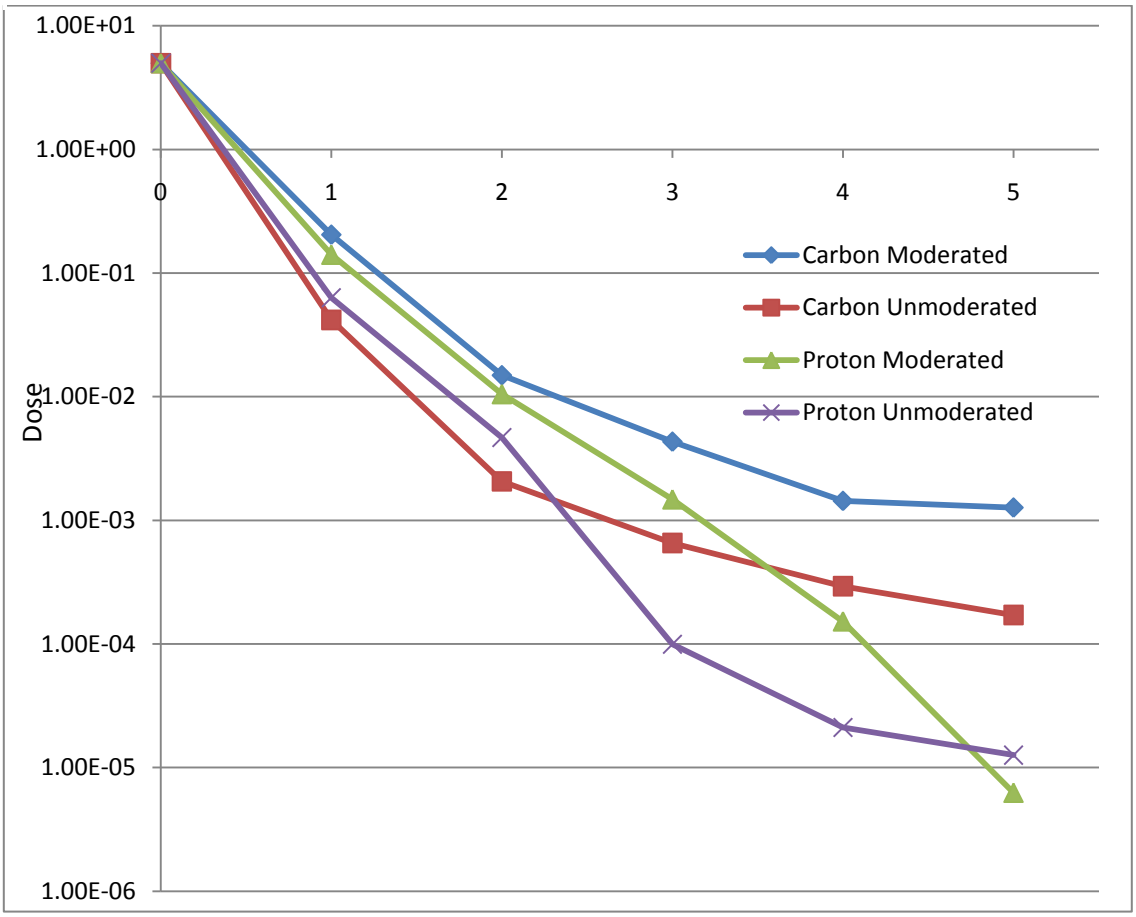

Fig. 8. Dose Delivered Perpendicular to the Tumor. Again, 0 is the tumor. 1-5 are regions 1-5 cm away laterally.

In this case, the moderated schemes have higher doses than the unmoderated schemes, but the dose is comparable for all beams. The proton schemes decrease more quickly than the carbon schemes at the 4-5 cm range.

For the carbon schemes only, fragmentation was also tallied. A tally was created that counted the number and type of particle at various points along the beam line. It was measured as the fraction of particles per source particle. Thus for carbon, it is a simple percentage remaining. For other particles, it is a measure of how many are created per initial carbon ion. A value of 0.5 for protons means that for every 2 carbon

ions in the initial beam, 1 proton was present at that point on the z axis. Thus, the higher the number, the more prevalent that particle was at that point on the axis. Fig. 9 shows the fragmentation of the moderated carbon beam.

In Fig. 9 carbon starts at about 80% of the initial fluence incident on the moderator, drops gradually to approximately 40%, and then falls off completely as it stops in the tumor. It is being replaced by its fragments, mostly alpha particles, followed by neutrons and protons. After all the carbon is stopped, new fragments from carbon are no longer being created (although large fragments such as alpha particles could fragment again), and the population of fragments begins to fall as they are stopped behind the target. Fig. 10 shows the same tally for an unmoderated carbon beam.

In Fig. 10, the beam begins as pure carbon. The population of fragments rises rapidly, however. At the end of its range, the beam is approximately 50% carbon remaining. The primary fragments are alphas, neutrons, and protons once again. Alpha particles are produced more slowly initially, but peak higher than protons and neutrons. All fragments begin to decrease beyond the target.

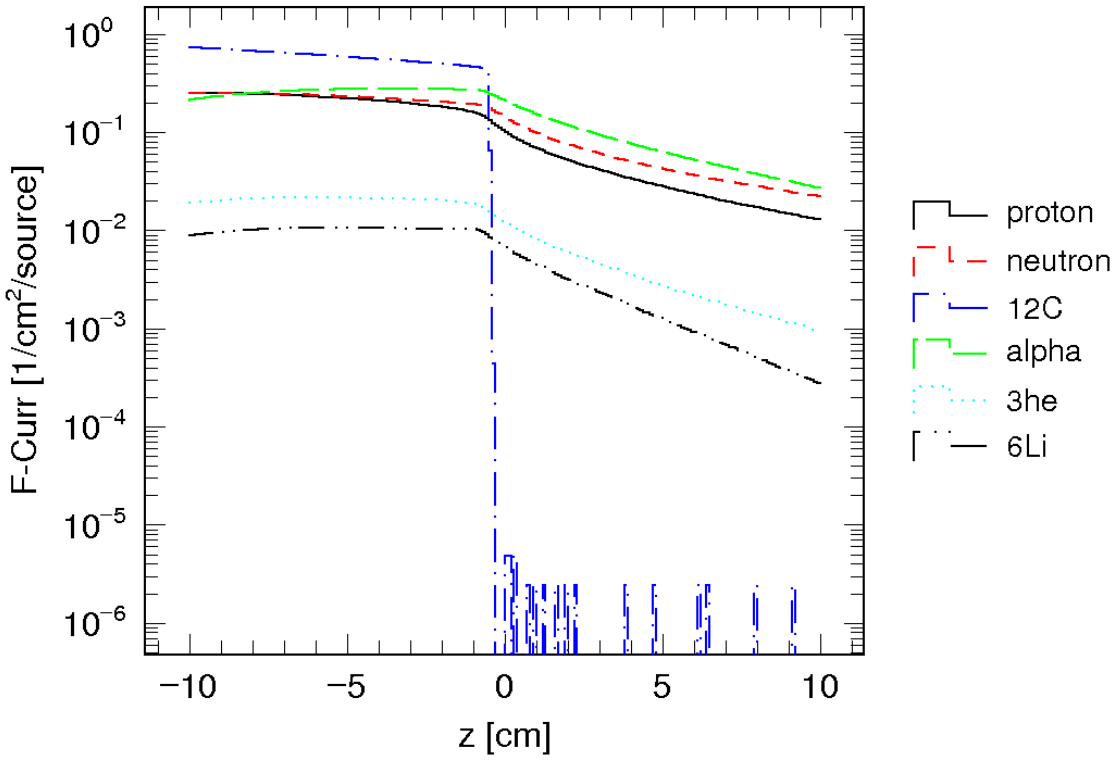

Fig. 9. Fragmentation of the Moderated Carbon Beam. F-curr is forward current. Forward current is the number of particles passing through along the forward z direction, divided by the area.

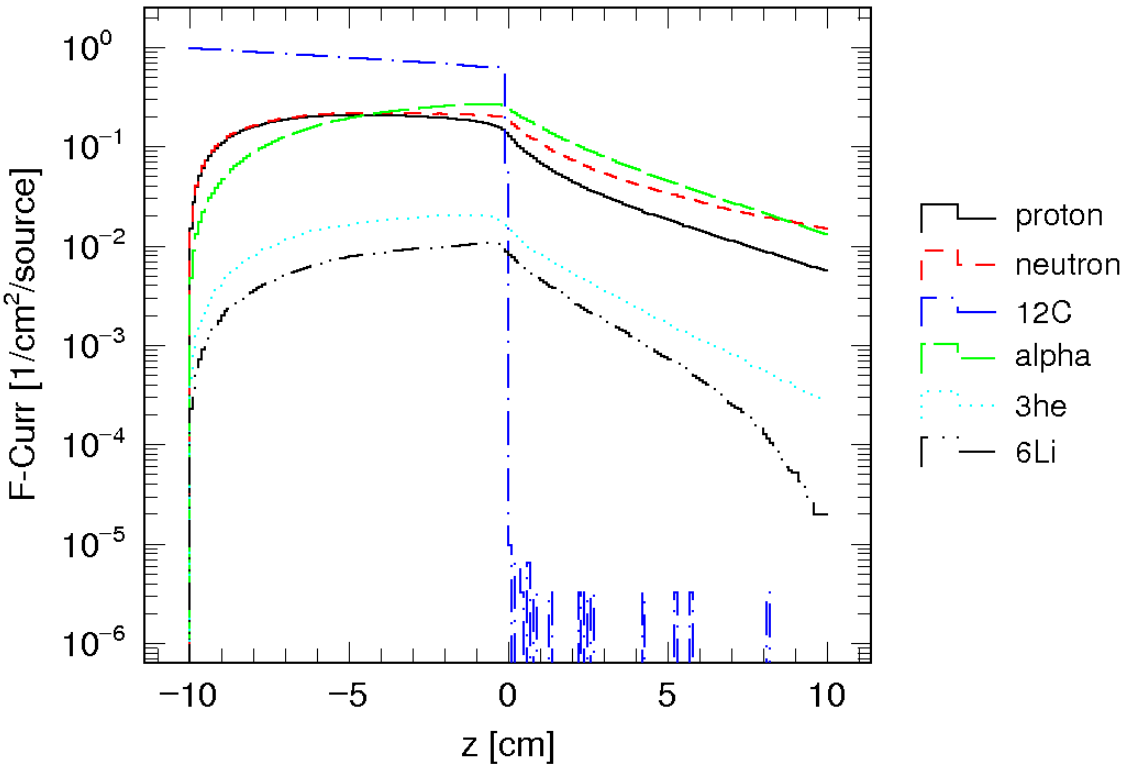

Fig. 10. Fragmentation of the Unmoderated Carbon Beam. Notice that the various fragments all begin at 0, unlike Fig. 9.

4. CONCLUSIONS

Fragmentation paints a very different picture of carbon ion beams than a simple Bragg peak analysis does. A Bragg peak seems to show that carbon ions deliver dose very precisely to a tumor, sparing surrounding tisssue. And indeed, the carbon ions themselves do stop precisely where they are intended to. However, half or more of them have been fragmented into smaller particles by the time they reach the target. These fragments have a range of energies and wider Bragg peaks. The neutron fragments are not charged particles, and deposit their energy over a wide area. These smaller particles are also more prone to scattering off of the beam line.

Carbon ions show a tighter beam at the treatment site than protons. They are less likely to scatter off at a large angle and deliver dose to healthy tissue off of the beam line. However, the dose to regions behind the tumor is much greater from a carbon beam. This may be the deciding factor in choosing carbon or proton beams. The dose to the first centimeter behind the tumor is more than 350 times greater (0.911 Gy for carbon, 0.00257 Gy for proton) for carbon compared to protons in the moderated setup. For the 2-5cm regions, and the unmoderated regimes, the difference is much greater.

For dose beside the tumor, the key factor was not particle type, but the presence or absence of a moderator. Both unmoderated beams delivered lower doses to the tissue laterally away from the beam line. However, the difference wasn't as large as those in the behind-tumor region. The proton beams also had lower doses at the farthest points, because the range of the protons was too short to reach those areas.

The fragmentation of carbon ions was decreased with the unmoderated beam. A significant degree of fragmentation occurred in the moderator itself, increasing the fragmentation of the beam at the tumor site. The dose from the umoderated beam was only one fifth of the moderated beam dose for all 5 regions behind the tumor. The unmoderated beam also tended to have less scattering; the dose to areas off the beam

line was significantly reduced. This strongly supports selcting beam energy in the accelerator instead of passing it through a physical moderator as a way of controlling the initial energy.

It is important to note that with the increased RBE of carbon within its Bragg peak, a lower dose could be used to deliver the same dose equivalent. If carbon's RBE compared to protons is 4, the dose could be lowered by a factor of 4. This would decrease the the dose behind the tumor due to fragments. The dose at 1cm behind was 350 times greater for carbon than it was for protons. A reduction by a factor of 4 still leaves a dose 75 times greater, at 0.23 Gy However, it also decreases entrance dose near the surface of the tissue by a factor of 4. Though complex, it would be worthwhile to compare the dose equivalents to healthy tissue of carbon and protons for a 5 Sv dose equivalent to the tumor. It may be that carbon offers an advantage in that sense. Or perhaps it's the case that carbon becomes better for sparing shallow tissue, but protons are better for sparing deep tissue. This could be a future line of inquiry.

REFERENCES

Attix FH. Introduction to Radiological Physics and Radiation Dosimetry. Weinheim, Germany: Wiley-VCH; 2004.

Durante M, Cucinotta FA. Heavy Ion Carcinogenesis and Human Space Exploration. Nat Rev Cancer. 8: 465-472; 2008.

Early PJ, Landa ER. Use of Therapeutic Radionuclides in Medicine. Health Phys 69: 677-694; 1995.

Hall EJ, Giaccia A . Radiobiology for the Radiologist. Philadelphia: Lippincott Williams & Wilkins; 2006.

Huff C. Catching the Proton Wave. [online] Available at: http://www.proton-therapy.org/hhnarticle.htm. Accessed June 1 2010.

International Atomic Energy Agency, International Commission on Radiation Units (IAEA/ICRU). Relative Biological Effectiveness in Ion Beam Therapy. Vienna: International Atomic Energy Agency; Technical Reports Series No. 461; 2008.

Imai R, Kamada T, Tsuji H, Yanagi T, Baba M, Miyamoto T, Kato S, Kandatsu S, Mizoe J, Tsuji H, Tatezaki S. Carbon Ion Radiotherapy for Unresectable Sacral Chordomas. Clin Cancer Res 10: 5741-5746; 2004.

Krishnanan S, Foote RL, Brown PD, Pollock BE, Link MJ, Garces YI. Radiosurgery for Cranial Base Chordomas and Chondrosarcomas. Neurosurgery 56: 777-784; 2005.

Niita, K. PHITS Ver. 2.08 User's Manual. Translated by H Iwase. Tokai, Japan. Research Organization for Information Science and Technology (RIST); 2006.

Particle Therapy Co-Operative Group (PTCOG). Hadron Therapy Patient Statistics [online].Available at: http://ptcog.web.psi.ch/Archive/Patientstatistics-update02Mar2009.pdf Accessed 25 August 2009.

Pawlik TM, Keyomarsi K. Role of Cell Cycle in Mediating Sensitivity to Radiotherapy. Int J Radiat Oncol Biol Phys 59: 928-942; 2004.

Rusin P, Walczak A, Zwierzchlejska A, Olszewski J, Morawiec-Bajda A, Kaczmarczyk D, Kusmierczyk K, Garncarek P, Pytel D, Sliwiński T, Majsterek I. DNA damage and repair of head and neck cancer cells after radio- and chemotherapy. Z Naturforsch C 64: 601-610; 2009.

Schardt D, Schall I, Geissel H, Irnich H, Kraft G, Magel A, Mohar MF, Munzenberg G, Nickel F, Scheidenberger C, Schwab W, Sihver L. Nuclear Fragmentation of High-Energy Heavy-Ion Beams in Water. Adv Space Res 17: 87-94; 1996

Schulz-Ertner D, Tsujii H. Particle Radiation Therapy Using Proton and Heavier Ion Beams. Am J Clin Oncol 25: 953-964; 2007.

Smathers JB, Otte VA, Smith AR, Almond PR, Attix FH, Spokas JJ, Quam WM, Goodman LJ. Composition of A-150 Tissue-Equivalent Plastic. Medical Phys 4: 74-77; 1977.

Souhami L, Olivier A, Podgorsak EB, Villemure JG, Pla M, Sadikot AF. Fractionated Stereotactic Radiation Therapy for Intracranial Tumors. Cancer 68: 2101-2108; 1991

Yamada S. New Carbon Therapy Project at Gunma-University Heavy-Ion Medical Center [online]. Available at: http://ptcog.web.psi.ch/PTCOG46/May%2023,%202007,%20afternoon/(58)- (5.23)(13.50)S.Yamada(New%20carbon%20therapy%20facility%20at%20Gunma%20University).pdf. Accessed 1 June 2010

Zamosky L. Partnering to Serve Patients and Save Dollars. Healthcare Financial Management Association. [online]. Available at: http://www.hfma.org/leadership/PartneringtoServe.html. Accessed 1 September 2009.

APPENDIX

PHITS CODE FOR MODERATED CARBON RUN

```
[ T i t l e ]
tumor stack

[ P a r a m e t e r s ]
 icntl   = 0
 maxcas  = 10000
 maxbch  = 100
 emin(1) = 0.0001          $ cut-off energy for proton (MeV)
 emin(2) = 0.0001                $ cut-off energy for neutron (MeV)
 emin(12) = 0.0001               $ cut-off energy for electron (MeV)
 emin(13) = 0.0001               $ cut-off energy for positron (MeV)
 emin(14) = 0.0001               $ cut-off energy for photon (MeV)
 emin(15) = 0.0001               $ cut-off energy for deuteron (MeV/n)
 emin(16) = 0.0001               $ cut-off energy for triton (MeV/n)
 emin(17) = 0.0001               $ cut-off energy for 3He (MeV/n)
 emin(18) = 0.0001               $ cut-off energy for alpha (MeV/n)
 emin(19) = 0.0001               $ cut-off energy for neucleus (MeV/n)
$ dmax(1) = 20.0           $ nuclear data max energy for proton (MeV)
$ dmax(2) = 20.0           $ nuclear data max energy for neutron (MeV)
$ dmax(12) = 1000.0             $ nuclear data max energy for electon (MeV)
$ dmax(13) = 1000.0        $ nuclear data max energy for positron (MeV)
$ dmax(14) = 1000.0             $ nuclear data max energy for photon (MeV)
 esmin = 0.00001           $ minimum energy for range calculation (MeV)
 igamma = 1                      $ 1: to use the gamma decay option
 itall = 1                 $ 1: to output tally evry batch
$ iggcm = 1                      $ 1: to output the GG warning echo back
$ ipara = 1                      $ 1: to output all parameter
$ igchk = 1                      $ 1: to check geometry
 file(6) = PHITS.out             $ file name of output summary
 $ file(7) = D:\PHITS2\PHITS213\library\mcnpxdata\xsdir        $ file name of nuclear data
  file(14)= C:\Users\Keel\Desktop\PHITS216\data\trxcrd.dat    $ file name of gamma decay data
 ides = 0                  $ 0: photon produces electron
 dircha = 1                      $ 1: for windows
$ irskip = 273900          $ for debug
$ rseed = 102645264135097   $ for debag
 nedisp = 1                      $ energy straggling option
```

```
 nspred = 1                          $ angular straggling option
 nlost = 200                  $ max number of lost particles
 emcnf = 20.0                 $ threshold of neutron capture
$ set:  M[ 27 ] rho[ 2.7 ] d[ 0.6 ] NA[ 6.0221367e-4 ]

[ S o u r c e ]
 s-type =  1
  proj = 12C
  x0 = 0.0
  y0 = 0.0
  z0 = -17.0
  z1 = -17.0
  r0 =  0.1
  dir = 1.0
  e0 = 290

[ M a t e r i a l ]
m1   13027  -2.7              $ aluminum
m2   14028  -2.2              $ silicon detector
m3   1001.60c   -0.102*(1.138)                  $ A-150
    6012.60c   -0.768*(1.138)
    7014.60c   -0.036*(1.138)
    8016.60c   -0.059*(1.138)
    9019.60c   -0.017*(1.138)
   20040.60c   -0.018*(1.138)

m4   1001.60c   2/3                  $ Ch2
    6012.60c   1/3


[ S u r f a c e ]
  1    RPP   -0.5 0.5 -0.5 0.5 -0.5 0.5
  2    cx    10
  3    px    10
  4    px    -10
  6    RPP   -5  5  -5  5  -16.5  -10.01
  7    so    25
  11    RPP   -0.5 0.5 -0.5 0.5 0.5 1.5   $11-15 are 1cc regions after tumor
  12    RPP   -0.5 0.5 -0.5 0.5 1.5 2.5
  13    RPP   -0.5 0.5 -0.5 0.5 2.5 3.5
  14    RPP   -0.5 0.5 -0.5 0.5 3.5 4.5
  15    RPP   -0.5 0.5 -0.5 0.5 4.5 5.5
```

```
 21   RPP   -0.5 0.5 0.5 1.5 -0.5 0.5  $21-25 are regions perpendicular to the beam line, aligned with
tumor
 22   RPP   -0.5 0.5 1.5 2.5 -0.5 0.5
 23   RPP   -0.5 0.5 2.5 3.5 -0.5 0.5
 24   RPP   -0.5 0.5 3.5 4.5 -0.5 0.5
 25   RPP   -0.5 0.5 4.5 5.5 -0.5 0.5
 31   RPP   -0.5 0.5 -0.5 0.5 -5.5 -4.5  $31 is a region 5 cmin front of the tumor
 41   RPP   -0.5 0.5 -0.5 0.5 -9.5 -8.5  $region near the surface of the tissue
 91   RPP   -0.5 0.5 -0.5 0.5 -16.5 -15.5 $region at the surface of the poly block


[ C e l l ]
 1  3  -1.0  -1                                  $ Tissue Sphere

 11 3  -1.0  -11
 12 3  -1.0  -12
 13 3  -1.0  -13
 14 3  -1.0  -14
 15 3  -1.0  -15

 21 3  -1.0  -21
 22 3  -1.0  -22
 23 3  -1.0  -23
 24 3  -1.0  -24
 25 3  -1.0  -25

 31 3  -1.0  -31

 41 3  -1.0  -41

 91 4  -0.94 -91

 2  3  -1.0  -2 +1 -3 4 11 12 13 14 15 21 22 23 24 25 31 41     $ Body Cylinder
 4  4  -0.94  -6 91                                  $ poly moderator


 5  0  -7    #1 #2 #4 #11 #12 #13 #14 #15 #21 #22 #23 #24 #25 #31 #41 #91      $ inside universe
 6  -1  7                                           $ outside universe



[ T - C r o s s ]
title = tumor crossing
```

```
mesh = reg
reg = 1
 r-in   r-out  area
  15      2      6.0
e-type = 2
 ne = 1
 emin = 0.1
 emax = 12000.0
unit = 1
axis = reg
file = tumor.cross.evt
factor = 1
output = f-curr
epsout = 1
dump = -2
  1 8

[ E N D ]

[ T - C r o s s ]
title = In-Beam Fragmentation
mesh = xyz
 x-type =  2
     nx =  1
   xmin = -0.5
   xmax =  0.5
 y-type =  2
     ny =  1
   ymin = -0.5
   ymax =  0.5
 z-type =  2
     nz =  200
   zmin = -10
   zmax =  10
part = 2212 2112 6000012 2000004 2000003 3000006
file = inbeam_frag
epsout = 1
axis = z
unit = 1
e-type = 2
 ne = 1
 emin = 0.0
 emax = 12000.0
```

```
output = f-curr


[ T - G s h o w ]
 title = Experiment Geometry
 mesh = xyz
  x-type =  2
     nx =  1
    xmin = -0.5
    xmax =  0.5
  y-type =  2
     ny =  400
    ymin = -20
    ymax =  20
  z-type =  2
     nz =  400
    zmin = -20
    zmax =  20
 axis = yz
 file = tumor.dat
 output = 4
epsout = 1

[T - H E A T ]
title = edep behind tumor
mesh = reg
reg = 1 11 12 13 14 15
file = behind.tumor.dat
epsout = 1
unit = 2
axis = reg

[T - H E A T ]
title = edep beside tumor
mesh = reg
reg = 1 21 22 23 24 25
file = perpindicular.tumor.dat
epsout = 1
unit = 2
axis = reg

[ T - C r o s s ]
title = tumor crossing
```

```
mesh = reg
reg = 1
 r-in   r-out  area
  1    (2 11)   6
e-type = 2
 ne = 1
 emin = 0.1
 emax = 12000.0
unit = 1
axis = reg
file = tumor.cross.evt
factor = 1
output = f-curr
epsout = 1
dump = -7
  1 2 3 4 8 18 19

 [ T - H E A T ]
title = edep z  mesh
mesh = xyz
 x-type =  2
    nx =  1
   xmin = -0.5
   xmax =  0.5
 y-type =  2
    ny =  400
   ymin = -10
   ymax =  10
 z-type =  2
    nz =  400
   zmin = -10
   zmax =  10


axis = yz
factor = 1
part = all
unit = 2
file = Tissue.depth.2d.p.dat
epsout = 1

[ T - H E A T ]
title = edep z  mesh
```

```
mesh = xyz
 x-type =  2
    nx =  1
  xmin = -0.5
  xmax =  0.5
 y-type =  2
    ny =  1
  ymin = -0.5
  ymax =  0.5
 z-type =  2
    nz =  200
  zmin = -10
  zmax =  10
axis = z
factor = 1
part = all
unit = 2
file = Tissue.depth.p.dat
epsout = 1
```

```
[ T - C r o s s ]
mesh = reg
reg = 1
 r-in   r-out     area
  11     12        6
part = all
e-type = 2
  ne = 1
  emin= 0.1
  emax = 12000
a-type = -1
 na= 9
  0 10 20 30 40 50 60 70 80 90
unit = 1
axis = the
file = angle.001
title = particle angle after tumor
output = a-curr
epsout = 1
```

```
[ T - C r o s s ]
mesh = reg
reg = 4
 r-in  r-out  area
  91   4      1
  41   2      1
  31   2      1
   1 (11 2)    1
part =  all 6000012
e-type =2
 ne = 1
 emin = 0.1
 emax = 12000
unit = 1
axis = reg
file = carbonleft.001
title = depletion of carbon in beam
output = current
epsout = 1


[ T - H e a t ]
title = Energy Deposited in tumor
mesh = reg
reg = 1
axis = eng
file = tumor.mod.p.dat
material = all
e-type = 2
 ne = 500
 emin = 0
 emax = 1000
output = deposit-all
unit = 3
epsout = 1
electron = 1


[ T - L E T ]
title = LET mesh
```

```
mesh = xyz
 x-type =  2
    nx =  1
  xmin = -1
  xmax =  1
 y-type =  2
    ny =  1
  ymin = -1
  ymax =  1
 z-type =  2
    nz =  500
  zmin = -10
  zmax =  10
part = all
l-type = 2
 nl = 700
 lmin = 0
 lmax = 1400
unit = 6
axis = z
file = Tissue.let.dat
epsout = 1

[ E n d ]

[ T - H e a t ]
title = Energy Deposited after tumor
mesh = reg
reg = 3
axis = eng
file = after.tumor.mod.p.dat
material = all
e-type = 2
 ne = 700
 emin = 0
 emax =1400
output = deposit-all
unit =     3
epsout = 1
electron = 1

[ T - C r o s s ]
title = fragments crossing last det
```

```
mesh = reg
reg = 1
 r-in   r-out  area
  15     14     6.45
e-type = 2
 ne = 1
 emin = 0.0
 emax = 1e9
unit = 1
axis = reg
file = CR39-cross-SiBack.dat
factor = 1
output = f-curr
epsout = 0
dump = -2
  1 8

$H.102                          $ muscle tissue
  $  C.123
  $  N.035
  $  O.729
  $  Na.0008
  $  Mg.0002
  $  P.002
  $  S.005
  $  K.003

  [ T - 3 D s h o w ]
    reg = all
    output = 3
    file = tumor.3d.dat
    epsout = 1
    w-dst = 50
  shadow = 2
```

VITA

Name:	Keel Brandon Curtis
Address:	Keel Curtis c/o Department of Nuclear Engineering Texas A&M University 3133 TAMU College Station, TX 77843-3133
Email address:	Keel.Curtis@gmail.com
Education:	B.S. Radiological Health Engineering, Texas A&M University, 2007 M.S. Health Physics, Texas A&M University, 2010